# NUMERICAL ANALYSIS OF THE VISCOELASTIC FLUID IN PLANE POISEUILLE FLOW

N. Khorasani and B. Mirzalou
[1]Department of Mechanical and Aerospace engineering, Science and Research Branch, Islamic Azad University, Tehran, Iran

***ABSTRACT***

*The state of flow parameters and bifurcation pictures is evaluated for the flow of a nonlinear viscoelastic fluid in a closed channel. The fluid's constitutive equation is assumed to be a derivative of Oldroyd-B and the flow is in between two parallel planes driven by a controlled pressure gradient. In simulation, a set of coupled ordinary differential equations with high degree of non-linearity is resulted. The shear stress/ shear rate curve of the fluid has a maximum and a minimum in the steady state condition. The velocity and stress are represented by orthogonal functions in the direction of the flow and transverse to it. The flow field is obtained from the conservation and constitutive equations truncated by Chebychev functions. Normal stress effects are also taken into account. The steady state and transient solutions are obtained for different Weissenberg numbers. It is observed that for a certain Weissenberg number, the system exchanges its stability with a deviation flow. At a second critical number however, the deviation flow diminishes. Finally, it is found that the flow responds oscillatorily when the Reynolds number is small, and monotically at large Reynolds number.*

***KEYWORDS:*** *Viscoelastic, Poiseuille flow, Johnson-Segalman, Galerkin, Chandrasekhar*

## I. INTRODUCTION

While the problem of PPF has been extensively investigated for Newtonian fluids, respectively little attention has been devoted to the flow of viscoelastic fluids especially Johnson-Segalman model. Laminar poiseuille flows have gained interest in the past two decades due to their applications in many processes involving liquid flows in relatively long tubes, such as waxy crude oil transport [1,2] and polymer extrusion [3,4]. Flow through a channel with fixed boundary conditions and the constant applied negative pressure gradient is known as the Poiseuille flow that contains viscoelastic fluid. Several constitutive equations, such as Doi-Edwards model with a rouse relaxation mode [5,6], the Gieskus model [7], The Maxwell and Oldroyd predict shear stress/ shear rate diagram behaviour, although the Johnson-Segalman model has non-monotonic curves. Theoretical studies on Couette and Poiseuille flows, using the more popular constitutive models, such as Maxwell fluids, found that the base flow is linearly stable at any level of elasticity, in the absence of inertia [8,9]. Recent experiments have shown that non-monotonic constitutive models are suitable to describe plane flows behaviour [10]. The Johnson-Segalman model is used for modelling a high molecular weight fluid composed of a Newtonian solvent and a polymer solute. It is predicted that the bifurcation diagram is influenced dramatically by the viscosity value. The present paper explores and analyses stress parameters and important factors of Johnson-Segalman fluid in a Poiseuille flow. Fluid elasticity and normal stresses give rise to additional nonlinearities and coupling among the flow variables, making an already complex problem even more difficult to solve. Because of this we should solve the equations with a more efficient numerical solution method that will be explained later.

The present study focuses on the steady state and pre-critical range of transient behaviour of the PPF of a JS fluid. Fluid elasticity and normal stresses give rise to additional nonlinearities and coupling among the flow variables, making an already complex problem even more difficult to solve. The interplay between inertia and elasticity was examined using a system of six degrees of freedom. A judicious mode selection was later carried out to include the dominant velocity and stress terms. The

results show good agreement with the behaviour based on the work of Ashrafi [11].Jeorgiou and Vlassopoulos [12] solved the time-dependant plane shear flow of a Johnson-Segalman fluid using mixed finite elements in space and a fully- implicit scheme in time. Their numerical results agree with findings of Kolkka et al. [13].The present work completes the work of Ashrafi and Khayat [14].

## II. PROBLEM FORMULATION

The plane-Poiseuille flow of a Johnson-Segalman fluid is formulated in this section. Consider a flow of an incompressible viscoelastic fluid of density ρ, relaxation time λ and viscosity η in a channel of width d. the x axis is parallel to the walls and is located exactly between the plates while the y axes is perpendicular to it and directs upward. Two boundary plates are constant and the applied pressure gradient drives the fluid toward in the closed channel. In this study, only fluids that can be reasonably represented by a single relaxation time and constant viscosity are considered. The fluid is a polymer solution composed of a Newtonian solvent and a polymer solute of viscosities $\eta_2$and$\eta_1$, respectively. Therefore $\eta = \eta_1 + \eta_2$. In general, the flow is governed by the continuity and conservation of momentum equations for an incompressible fluid with the applied constitutive equation of Johnson-Segalman model [15,16]. The JS model in dimensional form is given by:

$$\lambda\frac{\mathrm{D}\mathbf{T}}{\mathrm{Dt}} + \mathbf{T} = \eta_1[\nabla\mathbf{U} + (\nabla\mathbf{U})^{\mathrm{t}}] \tag{1}$$

$$\frac{\mathrm{D}\mathbf{T}}{\mathrm{Dt}} = \frac{\partial\mathbf{T}}{\partial\mathrm{t}} + \mathbf{U}.\nabla\mathbf{T} - \left(1-\frac{\zeta}{2}\right)((\nabla\mathbf{U})^{\mathrm{t}}.\mathbf{T} + \mathbf{T}.\nabla\mathbf{U}) + \frac{\zeta}{2}(\nabla\mathrm{U}.\mathrm{T} + \mathrm{T}.(\nabla\mathrm{U})^{\mathrm{t}}) \tag{2}$$

U is the velocity vector, P is the pressure, T is the polymeric contribution of the stress tensor, t is the time, $\boldsymbol{\nabla}$ is the gradient operator and $\zeta \in [0,2]$ is a dimensionless material (slip) parameter. Equation (2) includes both lower and upper-convective terms. The value of $\zeta$ is a measure of the contribution of non-affine motion to the stress tensor. For $\zeta = 0$ the motion is affine and the Oldroyd-B model is recovered, whereas for $\zeta = 2$, the motion is completely non-affine and the model is reduced to the Oldroyd-Jaumann model [17]. When $\zeta = 0$ and $\eta_2 = 0$, the upper-convected Maxwell model is recovered. Thus equation (1) belongs to the class of Oldroyd constitutive equations for incompressible viscoelastic fluids and can also be cast in terms of the Jaumann derivative [15]. After implementing the continuity and momentum equations with respect to the two above equations, a set of ODEs will be achieved:

$$\mathrm{Re}\,\frac{\partial\mathbf{u}}{\partial\mathrm{t}} = -\mathrm{We}\,\frac{\mathrm{dP}}{\mathrm{dx}} + \frac{\partial\boldsymbol{\tau}_{\mathrm{xy}}}{\partial\mathrm{y}} + \varepsilon\,\frac{\partial^2\mathbf{u}}{\partial\mathrm{y}^2} \tag{3}$$

$$\frac{\partial\boldsymbol{\tau}_{\mathrm{xx}}}{\partial\mathrm{t}} = -\boldsymbol{\tau}_{\mathrm{xx}} + (2-\zeta)\frac{\partial\mathbf{u}}{\partial\mathrm{y}}\boldsymbol{\tau}_{\mathrm{xy}} \tag{4}$$

$$\frac{\partial\boldsymbol{\tau}_{\mathrm{yy}}}{\partial\mathrm{t}} = -\boldsymbol{\tau}_{\mathrm{yy}} - \zeta\frac{\partial\mathbf{u}}{\partial\mathrm{y}}\boldsymbol{\tau}_{\mathrm{xy}} \tag{5}$$

$$\frac{\partial\tau_{\mathrm{xy}}}{\partial\mathrm{t}} = -\tau_{\mathrm{xy}} + \frac{\partial\mathrm{u}}{\partial\mathrm{y}} - \frac{\zeta}{2}\frac{\partial\mathrm{u}}{\partial\mathrm{y}}\tau_{\mathrm{xx}} + \left(1-\frac{\zeta}{2}\right)\frac{\partial\mathrm{u}}{\partial\mathrm{y}}\tau_{\mathrm{yy}} \tag{6}$$

Here, the Reynolds number, Re, the Weissenberg number, We, and the solvent-to-solute viscosity ratio, $\varepsilon$, are the three similarity groups of the problem, which are given respectively by

$$\mathrm{Re} = \frac{\mathrm{d}^2\rho}{\eta_1\lambda} \quad , \quad \mathrm{We} = \frac{\mathrm{U}\lambda}{\mathrm{d}} \quad , \quad \varepsilon = \frac{\eta_2}{\eta_1} \tag{7}$$

U is the maximum velocity of the basic poiseuille flow at the axis of the channel. Note that in the case of$\frac{\mathrm{dp}}{\mathrm{dx}} = -1$, the first term of equation (3) turns out to be simply equivalent to the We number. The boundary condition is defined as:

(8)

$$\mathbf{u}\left(y = \mp\frac{1}{2}, t\right) = 0$$

Equations (3) to (6) are further simplified if they are cast in terms of the normal stress difference, N, and a combination of normal stresses, Z. the last is found to decay exponentially with time and exhibits uninteresting transient behavior and will be set equal to zero.

$$N = \tau_{xx} - \tau_{yy}, Z = \frac{\zeta}{2}\tau_{xx} + (1 - \frac{\zeta}{2})\tau_{yy} \tag{9}$$

It is convenient to seek the departure in velocity $u'$ and stress $\tau'_{ij}$ from the base flow, which are introduced as follows:

$$u = u^b + u', \tau_{ij} = \tau^b_{ij} + \tau'_{ij} \tag{10}$$

In this case the relevant equations become

$$Re\frac{\partial u}{\partial t} = \frac{\partial S}{\partial y} + \frac{\partial S^b}{\partial y} + \varepsilon\frac{\partial^2 u}{\partial y^2} \tag{11}$$

$$\frac{\partial N}{\partial t} = -N + 2(AyS + \frac{\partial u}{\partial y}S^b + \frac{\partial u}{\partial y}S) \tag{12}$$

$$\frac{\partial S}{\partial t} = -S + \frac{\partial u}{\partial y} + \alpha(AyN + \frac{\partial u}{\partial y}N^b + \frac{\partial u}{\partial y}N) \tag{13}$$

Note that the "Prime" is droped in above Equations. Below parameters are carried out from the base flow solution. In this paper, the index b refers to the base flow.

$$\frac{\partial u^b}{\partial y} = Ay \tag{14}$$

$$N^b = \frac{2(\frac{\partial u^b}{\partial y})^2}{1 + \zeta(2 - \zeta)(\frac{\partial u^b}{\partial y})^2} \tag{15}$$

$$S^b = \frac{\frac{\partial u^b}{\partial y}}{1 + \zeta(2 - \zeta)(\frac{\partial u^b}{\partial y})^2} \tag{16}$$

The following abbreviations, used in the equations, are introduced:

$$\alpha = \zeta(\frac{\zeta}{2} - 1) \tag{17}$$

$$A = \frac{We}{\varepsilon}\frac{dp}{dx} \tag{18}$$

## 2.1. Galerkin projection method and the dynamical system

The solution of Equations (11) to (13) is carried out using the Galerkin projection method. Similarly to any flow in the transition regime, the PPF of viscoelastic fluids involves a continuous range of excited spatio-temporal scales. In order to assess the effect of the motion of the arbitrarily many smaller length and time scales, one would have to resolve in detail the motion of the small scales. This issue remains unresolved, since despite the great advances in storage and speed of modern computers, it will not be possible to resolve all of the continuous ranges of scales in the transition regime. Because of this, nowadays, low order dynamical systems can be a viable alternative to conventional numerical methods to probe the nonlinear range of flow behaviour [18,19]. Low order dynamical systems are carried out using Galerkin projection method. The velocity and stress components assume

truncated Fourier or other orthogonal representations in space, depending on the boundary conditions. Expansion coefficients are functions of time alone, thus leading to a nonlinear system upon projection of equations onto the various modes. In this method the variables u(y,t), N(y,t) and S(y,t) are represented by series of Chandrasekhar functions that satisfy the homogenous boundary conditions. The suitable level of truncation that is imposed here, is M=2 that leads to a six-dimensional model. The general series representation for the velocity and normal stress difference are given by Equations (19) to (21).

$$u(y,t) = \sum_{i=1}^{M} u_i(t)\emptyset_i(y) \tag{19}$$

$$N(y,t) = \sum_{i=1}^{M} N_i(t)\emptyset_i(y) \tag{20}$$

$$S(y,t) = \sum_{i=1}^{M} S_i(t)\emptyset_i'(y) \tag{21}$$

Where $\emptyset_i(y)$ are the even and odd Chandrasekhar functions, for i even and odd, respectively [20], and $\emptyset_i'(y)$ are defined: $\emptyset_i'(y) = \frac{1}{\alpha_i}\frac{d\emptyset_i}{dy}$ , where $\alpha_i$ are constants. M is the number of modes. Finally after applying the Galerkin projection method on the equations, a set of six ODEs are generated and solved.

## III. RESULT & DISCUSSION

### 3.1. Steady state solution and bifurcation pictures

In this section, the steady-state solution is obtained for any parameter range and some limit cases will be considered in detail. The steady-state solution of equations (11) to (13) are derived by setting the time derivatives equal to zero. Equation (16) is the most revealing result of the poiseuille flow of the JS model. It reflects the possibility of non-monotonic behaviour for the stress/shear rate relation. Figure 1 shows the behaviour of the shear stress $\tau_{xy}^{b}$ as a function of $\frac{du}{dy}$ for $\zeta = 0.2$and $\varepsilon \in [0,1]$. The figure indicates that the stress curves tend to have two extrema, which merge as ε increases. This situation is reminiscent of the load/deformation behaviour in elasticity. The case of an Oldroyd-B fluid ($\varepsilon = 0$) is similar to the case of Neo-Hookean solid and the curve for a Newtonian fluid ($\varepsilon = 1$) is similar to a curve of a Hookean solid.

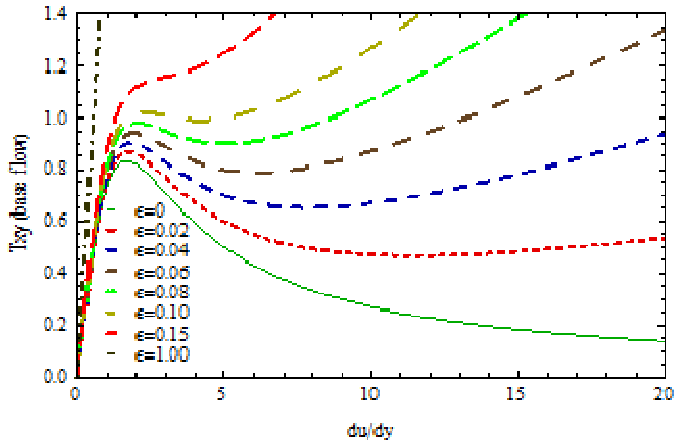


**Figure 1.** Steady-state shear stress/shear rate diagram for $\zeta = 0.2$and $\varepsilon \in [0,1]$.

Obtaining the bifurcation pictures for different values of *We* and $\zeta$ is very difficult and the resulted ordinary differential equations has resolved using a powerful software, spending a lot of time. Recall that the *Re* number, affect only the transient solution and does not take important role in the steady-state solution. Figure 3 and 4 show the steady-state normal and shear stresses value as a function of

$We \in [0,7]$for $\zeta \in [0.2,1]$. It has been shown that for$\zeta = 0$, the curves are linear and the system behaviour tends to the Newtonian fluid. With respect to the initial part of Figure 2, the system loses its stability much fasterat a certain *We*, as $\zeta$ increases and in fact the separation occurs earlier. All the curves start at the origin point. It is apparent from the figures that, in the phase spacethe base flow solution separates in to three parts: pre-critical region ($We < We_{c1}$), Critical region ($We_{c1} < We < We_{c2}$) and post-critical region ($We > We_{c2}$). The range of first critical *We* value is $We \in [0.4\,, 0.6]$ and the second range is $We \in [4.8\,, 5]$. For the critical range, an additional fixed branch emerges, which coincides with the loss of stability of the base flow and the emergence of a stable nonlinear velocity profile. These figures are symmetric with respect to the horizontal axis. By applying departures in velocity and stress, one sudden extremum at the beginning part ofthe curves in the Figure 3 occurs. This figure is comparable to those in Ref. [21]. Shear stress at the start of the motion is very high due to sudden applied pressure gradient and decreases after. It is obvious that there is a nonlinear relation between increasing$\zeta$ and the value of normal or shear stresses. While the grow steps of $\zeta$are equal to 0.2, with increasing this number, stress value decreases much slower.

### 3.2. Pre-critical transient behaviour

Numerical solution of Equations (11) to (13) with the mentioned method, leads to a nonlinear transient solution of the system. Chandrasekhar series representation is used to introduce the flow field and stress along with the Galerkin projection, to drive dynamical system that governs the expansion coefficients. All results of this section, belongs to the pre-critical *We* number. In this region the base flow is unconditionally stable [18]. The Reynolds number is fixed at *Re=0.1* and *We* is assumed to equal to 0.2. Transient flow behaviour of the system has been shown in the Figure 4. The departure of system to the base flow is shown with dimensionless time scales. In this region, the velocity profile is similar to the Newtonian Poiseuille flow but the curves slightly deviate from the central symmetry axis. Considering the parameters $\Delta p = -1.1$and $Re = 0.1$, it has been observed from the figure that until the time t=1.9, the velocity profile is rapidly increasing but after that, the growth of the velocity profile has stopped and the curves tend to steady-state condition. From this time to t=3.9, velocity magnitude has slightly reduced and finally at the mentioned time, the system is completely steady. Black dashed curve shows the final steady-state condition. Figure 5 indicates that, the flow does not converge monotonically towards the poiseuille base flow. There is in fact an oscillatory behaviour about the origin (base flow). According to the figure, the flow tends to grow in amplitude at the early stages, exceeding the initial amplitude. After that, the curves are damped after some oscillations according to the implemented pressure gradient value and the steady state velocity is attained approximately at t=5.5. it can be mentioned that while the Re number is constant, the applied pressure gradient do not affect the system to reach steady-state condition. In this region, with increasing the pressure gradient, the maximum velocity increases rapidly. However, due to the high complexity and the direct and indirect influence of this parameter in terms of obtained equations, this is not always true. For example, as is observed in the critical range analysis, transverse behaviour happens. The pressure that is imposed to the system, force the flow to move towards the uniform flow. Figure 6 shows the 3-dimensional transient behaviour of flow in the pre-critical range. The oscillating behaviour of the profile is clearly shown in the figure. The oscillations near axis of the channel are much more than near the walls. This figure gives an appropriate general side to review the flow parameters and velocity distribution in the channel.

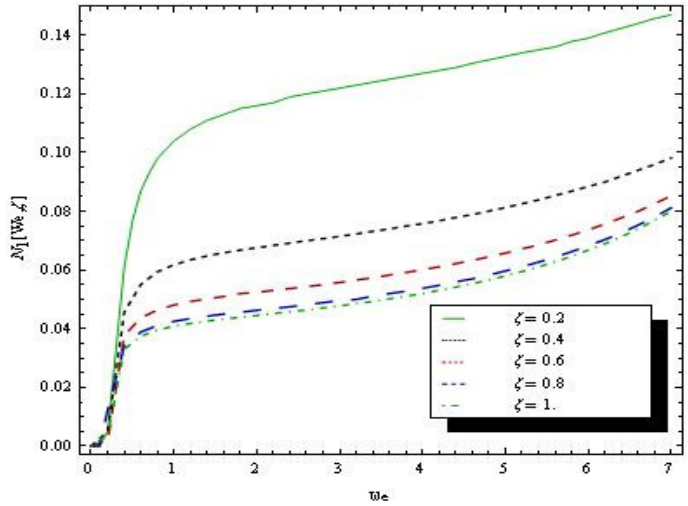


**Figure 2.** Bifurcation picture for normal Stress N as function of *We* for $\varepsilon = 0.04$,$Re = 0.5$, $\Delta p = -1$

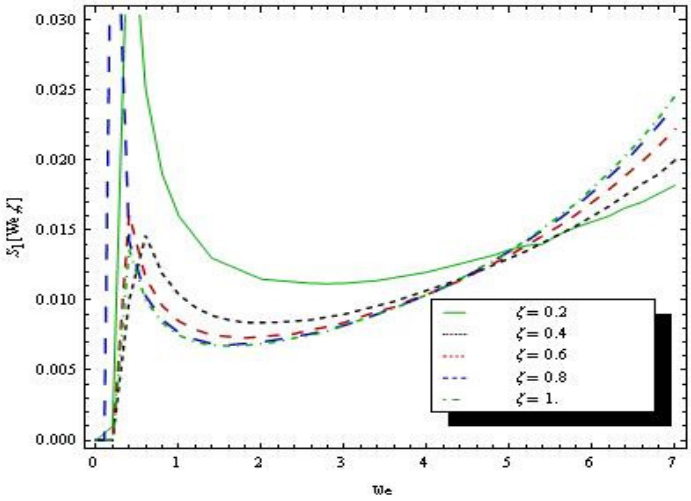


**Figure 3.** Bifurcation picture for shear Stress S as function of *We* for $\varepsilon = 0.04$,$Re = 0.5$, $\Delta p = -1$

Figure 7 shows the velocity profile against the time for$\varepsilon = 0.04$, $\zeta = 0.2$ and *We=0.2* at three different Reynolds number, respectively Re= 0.01, Re= 0.1and Re= 0.5. In the pre-critical Region, increasing pressure gradient of the system, increases the velocity and consequently stress value and the system attains the steady-state condition after some oscillations. There is a slight overshoot initially but the monotonous decay toward the steady state is obvious. Less oscillation occurs at a constant Reynolds number to reach the steady state condition, when the applied pressure gradient decreases and the fluid uniforms with less oscillation but at the same time as previous. The time to attain steady-state condition is independent of the pressure gradient. Number of oscillations is directly in related with the Reynolds number. The curve, depicted at Re=0.5 has less oscillations in comparison with the figure that is depicted in Re=0.1 but needs more time to uniform. For small Re, the convergence to the steady state is monotonic and quick as a result of the dominant viscous effects. Typically at small Re, there is a strong overshoot near t=0, which particularly forces the motion to be monotonic soon afterwards.

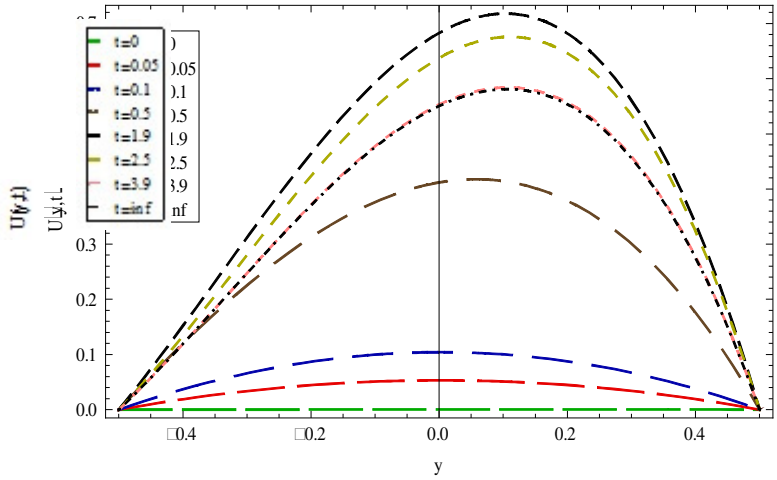


**Figure 4.** Transient behaviour of flow in the pre-critical range ($We < We_{c1}$) for $Re = 0.1, We = 0.2$ ، $\Delta p = -1.1, \varepsilon = 0.04$and$\zeta = 0.2$

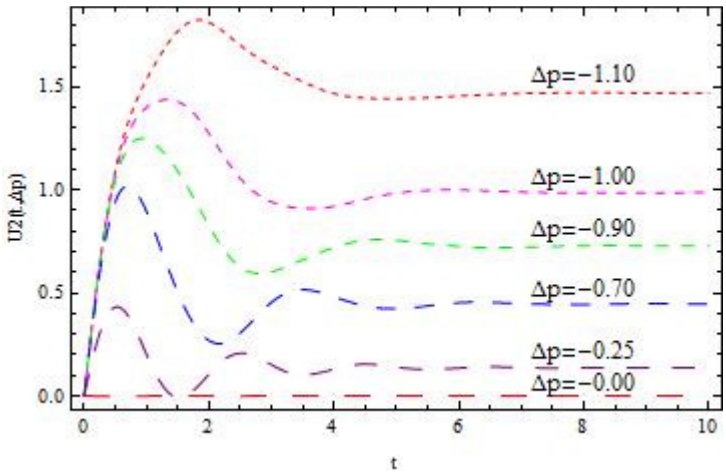


**Figure 5.** Influence of implemented pressure gradient on the velocity profile against the time in the pre-critical range ($We < We_{c1}$) for $Re = 0.1, We = 0.2, \varepsilon = 0.04$and$\zeta = 0.2$

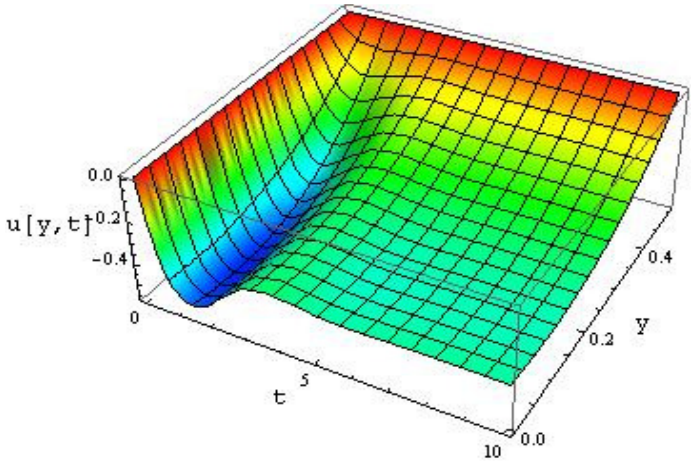


**Figure 6.** 3-dimensional transient behaviour of flow in the pre-critical range ($We < We_{c1}$) for $Re = 0.1$, $We = 0.2, \varepsilon = 0.04$ and $\zeta = 0.2$

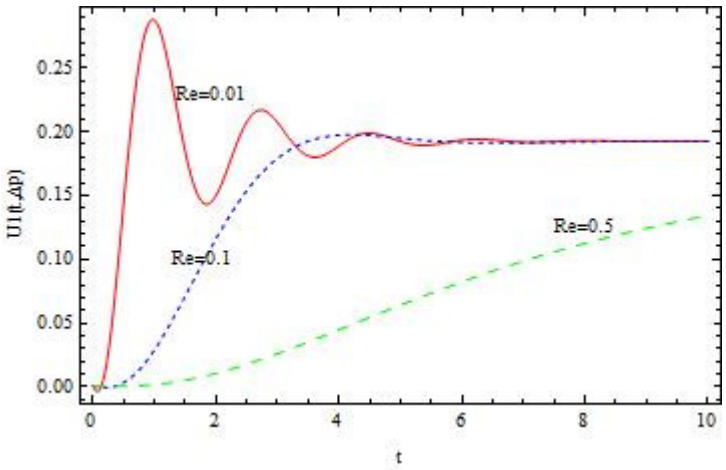


**Figure 7.** Transient flow curves at different Reynolds number for$\Delta p = -10, \varepsilon = 0.04$ and $\zeta = 0.2$

## IV. CONCLUSIONS

The steady state and transient nonlinear responses are examined for the plane-poiseuille flow of a viscoelastic fluid that obeys the Johnson-Segalman constitutive equation with added Newtonian viscosity. Given the complexity of the constitutive equation and the potentially intricate interplay between fluid inertia and elasticity, only one-dimensional disturbances are considered. Four dimensionless groups emerge in the formulation, namely, the Reynolds number, *Re*, the Weissenberg number, *We*, the solvent-to-solute viscosity ratio, $\varepsilon$, and the slip parameter, $\zeta$, in the constitutive model. A dynamical system approach based on the Galerkin projection method is adopted to describe the flow as *Re* and *We* are varied. The nonlinear dynamical system is derived by expanding the flow field (velocity and stress) into odd and even Chandrasekhar functions along the direction perpendicular to the flow. The equations governing the time-dependent expansion coefficients are derived by projecting the various modes onto the original equations. A suitable truncation level is adopted to close the hierarchy of the resulting set of ordinary differential equations. The stress curves tend to have two extrema, which merge as $\varepsilon$ increases. This situation is reminiscent of the load/deformation behavior in elasticity.

For given $\zeta$ and $\varepsilon$, two critical values of the Weissenberg number are found, at which an exchange of slopes and system behaviour takes place between the base flow and a non-trivial steady state branch (nonlinear velocity profile). The two critical points coincide with the extrema of the shear stress/shear rate curve. There are thus three ranges of Weissenberg numbers of interest that are investigated, namely, the pre-critical range, the critical range and the post critical range. Here, we consider only the pre-critical range in the transition regime that is always stable. Although the Reynolds number does not influence the value of the critical *We* numbers and the bifurcation picture, it has a significant influence on the transient behaviour. The time that the system attains steady state condition is independent of the applied pressure gradient. Number of oscillations is in related with the Reynolds number. For small *Re*, the convergence to the steady state is monotonic and quick as a result of the dominant viscous effects. Typically there is a strong overshoot near t=0, which particularly forces the motion to be monotonic soon afterwards. As the pressure gradient of the system increases, the magnitude of the stress will be increased and the system attains the steady state condition after some oscillations. There is a slight overshoot initially but the monotonous decay toward the steady state is obvious. Less oscillation occur at a constant Reynolds number to attain the steady state condition, when the applied pressure gradient decreases and the fluid uniforms with less oscillation but at the same time as previous. Various scenarios are explored to understand transient and nonlinear behaviour by varying *Re* and *We*. The results are depicted in Figures 4 to 7, where the flow in the pre-critical range of *We* is investigated. By increasing the Reynolds number, the flow takes more time to reach the steady-state condition. Thus the more viscous fluids, for a given level of elasticity, tend to relax faster.

## REFERENCES

[1]. G. Viney, A. Wachs, J. F. Agassant, (2006),"Numerical simulation of weakly compressible flows: the restart of pipeline flows of waxy crude oils", J. Non-Newtonian, Fluid Mech. 136 (2006)93-105.
[2]. M. R. Davidson, Q. D. Nguyen, H. P. Ronningsen, (2007), "Restart model for a multi-plug gelled waxed oil pipeline", J. petrol. Sci. Eng.59 (2007) 1-16.
[3]. G. C. Georgiou, M. J. Crochet, (1994), "Compressible viscous flow in slits with slip at the wall", J. Rheology, 38 (1994) 639-654.
[4]. G. C. Georgiou, (2003), "The time dependent compressible poiseuille and extrudate-swell flows of a carreau fluid with slip at the wall", J. Non-Newtonian Fluid Mech.109 (2003)93-114.
[5]. T. C. B Mcleish, R. C. Ball, (1986), J. polym. Sci. B 24(1986) 1375-1745
[6]. T. C. B. Mcleish, (1987), J. Poly. Sci. B 25, 2253-2264
[7]. D. S. Malkus, J. A. Nohel, B. J. Plohr, (1993), Proc. IUTAMsymp, "Numerical simulation of non-isothermal flow of viscoelastic fluids", vol. 28,pp.57-71
[8]. M. M. Denn, (1990), "Issuesin viscoelastic instability", Annu. Rev. Fluid mech. 22,13
[9]. R. G. Larson, (1992), "Instabilities in viscoelastic flows", Rheol. Acta 31, 213
[10] N. A. Spenley, X. F. Yuan, M. E. Cates, (1996), J. Phys.И. France 6, 551-571
[11] N.Ashrafi, (1999), "A low order dynamical systems approach to non-linear stability of non-Newtonian fluids", Doctorate Thesis, London
[12] G.C.Georgiou, D. Vlassopoulos, (1998), J. Non-Newtonian Fluid Mech. 75, 77-97
[13] R.W.Kolkka, D.S.Malkus, M.G.Hansen, G.R.Ierley,R.A.Worthing, (1998), J. Non-Newtonian Fluid Mech, 29, 303-335
[14] Roger E. khayat, NarimanAshrafi, (2002), "A low Dimensional approach to nonlinear plane-poiseuille flow of viscoelastic fluids"
[15] R. B. Bird, R. C. Armstrong, O. hassager, (1987), "Dynamics of polymeric fluids", 2nd edition, Wiley, NewYork, Vol. 1
[16] M. W. Johnson , D. Segalman, (1977), "A model for viscoelastic fluid behavior which allows non-affine deformation", J. Non-Newtonian fluid mech.2, 278
[17] M. W. Johnson , D. Segalman, (1977), "A model for viscoelastic fluid behavior which allows non-affine deformation", J. Non-Newtonian fluid mech.2, 278
[18] G.R.Sell, C.Foias and R.Temam, (1993), "Turbulance in Fluid flows: A dynamical system approach", Springer-Verlag,New York
[19]P.Holmes, J.L.Lumley, G.Berkooz, (1996), "Turbulance Coherent structures Dynamical systems and symmetry", Cambridge
[20] A. H. Nayfeh and B. Balachadran, (1995), "Applied Nonlinear Dynamics", John Wiley & Sons, New York
[21] Roger E.khayat, N. Ashrafi, (2002), "A low-dimensional approach to non-linear plane-Poiseuille flow of viscoelastic fluids",J. Physcs of fluids, Vol 14, 1757-1766

**Authors**

**Nariman Khorasani** is an assistant professor in Islamic Azad University, Science and Research branch, Tehran, Iran since 2005. He teaches graduate and undergraduate courses. His research area is Non-Newtonian flow.

**Babak Mirzalou** received the B.Sc. degree in Mechanical engineering from Bahonar University, Kerman, Iran, in 2009, The M.Sc. degree in Mechanical engineering from Science and Research branch of Islamic Azad University, Tehran, Iran, in 2012. His research interests include Non-Newtonian fluids and Rheology.